GCA Technical Report No. 63-25-N

66p.

INVESTIGATION OF THE INFLUENCE OF WINDS IN THE LOWER IONOSPHERE

L. G. SMITH

GEOPHYSICS CORPORATION OF AMERICA BEDFORD, MASSACHUSETTS

FINAL REPORT

CONTRACT NO. NASw-489

PREPARED FOR
NATIONAL AERONAUTICS AND SPACE ADMINISTRATION
WASHINGTON 25, D. C.

AUGUST 1963

GCA Technical Report No. 63-25-N

INVESTIGATION OF THE INFLUENCE OF WINDS IN THE LOWER IONOSPHERE

Leslie G. Smith

August 1963 66p

Final Report

(NASA Contract No. NASw-489)

(NASA CR-55105; GCA-TR-63-25-N) OTS: $6.60 ph, $2.18 mf

GEOPHYSICS CORPORATION OF AMERICA
Bedford, Massachusetts

Prepared for

NATIONAL AERONAUTICS AND SPACE ADMINISTRATION
Washington 25, D.C.

TABLE OF CONTENTS

Section	Title	Page
1	INTRODUCTION	1
2	SPORADIC-E LAYER	4
3	EXPERIMENTAL PROGRAM	10
	3.1 Payload	10
	3.2 Flight Summary	17
	3.3 Vehicle Performance	24
	3.4 Spin Stabilization	27
4	OBSERVATIONS	29
	4.1 Electron Density and Wind Structure	29
	4.2 Electron Temperature	39
	4.3 Measurements in the D Region	41
5	CONCLUSIONS AND RECOMMENDATIONS	45
	REFERENCES	49
	APPENDIX A	50
	APPENDIX B	60

SECTION 1

INTRODUCTION

The development of a measuring technique, based on the Langmuir probe, has provided a valuable new instrument for ionospheric investigation.[1-1] Two flights made on an earlier contract (NASw-98) demonstrated the feasibility of studying the fine structure of the electron density profile in the E layer.[1-2] In particular it was found that the thin layers of high electron density responsible for sporadic-E echoes on an ionosonde could be readily observed by sounding rockets and it became feasible to plan direct measurements aimed at determining the cause of this remarkable phenomenon.

It has recently been proposed by Whitehead[1-3] that occurrence of wind shears in the ionosphere could produce thin layers of high electron density. It also happened that more-or-less regular measurements were being made of the wind structure in the lower ionosphere using the sodium vapor trail method. It was therefore decided that a direct test of Whitehead's theory was possible and this program was the result.

In addition to an investigation of the role of wind shears in the formation of sporadic E the three rocket flights had other objectives, some being of a scientific nature while others relate to the vehicles and anticipated problems which concerned a subsequent contract (NASw-500). The scientific objectives were modified from those stated in the original proposal due to difficulties of scheduling the rocket flights, principally due to delays caused by unsuitable weather conditions. Also the performance of the three rockets was rather poor and they failed to reach the predicted altitude. However the principal objective was completed satisfactorily and a relationship between sporadic E and wind shear established.

The rocket flights were used to test a new method of trajectory determination for small sounding rockets based on the time-of-flight above a known altitude (greater than second-stage burnout). This method was subsequently used effectively at Fort Churchill, Manitoba, during the eclipse of 20 July 1963, where, as expected, the radar equipment was inadequate for skin-tracking the smaller rockets.

The launch times and main features of the three rocket flights which comprise this program are as follows. All launches were from Wallops Island, Virginia.

(1) Nike-Cajun 10.99, 0525 EST, 7 November 1962. An intense layer of sporadic E was penetrated at 100km. Otherwise this was a typical nighttime profile. The wind structure was observed 28 minutes later.

(2) Nike-Cajun 10.108, 0557 EST, 30 November 1962. The electron density profile on this occasion showed rather less irregular structure

than previous nighttime measurements. The ionosonde indicated a disturbed ionosphere at the time. The wind structure was measured 18 minutes later.

(3) Nike-Cajun 10.109, 1700 EST, 5 December 1962. This measurement at sunset showed an irregular electron density profile characteristic of the nighttime observations. The wind structure was measured 16 minutes later.

Two technical reports have been issued:

(1) "A Simple Method of Trajectory Determination for Sounding Rockets", L. G. Smith, GCA Technical Report No. 63-9-N, March 1963.

(2) "Measurements of Electron Density Profile in the Nighttime E Region", L. G. Smith, GCA Technical Report 63-22-N, June 1963.
Most of the material from these reports is included in the present report.

In addition the theory and operation of the measuring technique has been described in the following report:
"A DC Probe for Rocket Measurements in the Ionosphere", L. G. Smith, GCA Technical Report No. 63-19-N, June 1963. This report should be consulted for details of the instrumentation of the rockets.

SECTION 2

SPORADIC-E LAYER

This most interesting feature of the E region of the ionosphere has been recognized from the earliest studies of the region. The sporadic-E layer, which forms at about the same height as the normal E layer, is highly irregular (hence its name) and correspondingly unpredictable. It has no practical value in normal radio communication but has always been regarded with great interest as a major feature of the ionosphere. No entirely satisfactory explanation has yet been given of the formation of the layer but investigations such as that described in this report have indicated the value of sounding rockets in identifying the mechanism.

The sporadic-E echo on an ionosonde is defined by one or more of the following characteristics:

(1) Random time of occurrence;

(2) Partial transparency;

(3) Variation of penetration frequency with transmitter power;

(4) Reflection height independant of frequency.

The sporadic-E echo on an ionosonde is characterized by two frequencies f_bE_s and f_oE_s. The latter is the highest frequency at which an echo

is obtained; f_bE_s is the highest frequency at which the sporadic-E layer is opaque, as judged by the absence of any echo from the higher layers. In the frequency interval between f_bE_s and f_oE_s the sporadic-E layer is transparent and echoes can be seen from the higher layers in addition to the sporadic-E echo. The most interesting difference in the two quantities is in their variation with latitude. The incidence of sporadic E (as given by f_oE_s) increased markedly in a narrow zone centered on the geomagnetic equator. The "blanketing" frequency f_bE_s, on the other hand, shows a much smaller effect near the equator.

The greatest part of the body of knowledge about the occurrence and nature of sporadic E is based on data from ionosondes. More recently two other techniques have been used to supplement the original radio (vertical) sounding. These are the back-scatter technique and the various rocket-borne probing techniques. The great value of these is that they complement each other. The ionosonde is most valuable for the accumulation of statistics on the occurrence of sporadic E by time and place and also on the height of the layer. The back-scatter technique, used at fixed-frequency, gives a map of the layer and shows the movement. Rockets are most valuable for giving detailed information of the electron density profile of the layer.

These techniques give a picture of the sproadic-E layer in the temperate zone as thin clouds or patches of high electron density apparently moving with considerable velocity. The thickness of the layer is about 1 km, usually occurring close to 100 km altitude. The cloud has an average

diameter of about 200 km and velocity about 60 m/sec.[2-1] These properties define a type of sporadic E against which other types may be compared.

At geomagnetic latitudes greater than 60^{o} the duirnal variation is in opposite phase to that of the mid-latitudes. Thus auroral zone sporadic E shows a daily maximum shortly before midnight while the corresponding time in the temperate zone is shortly before noon. Again, the auroral zone sporadic E shows little seasonal variation in contrast to the marked preference for the summer months which is observed in the temperate zone. Most important the sporadic-E incidence in the auroral zone is positively correlated with magnetic activity i.e., it shows a (strong) preference for disturbed days whereas in the temperate zone sporadic E shows a (weak) preference for quiet days.

In the equatorial zone, which is defined to be the region near the equator with a dip-angle of less than 5^{o}, the incidence of sporadic E is remarkably high during the hours of daylight and falls off sharply at night. There is no marked seasonal variation.

On an ionosonde the sporadic-E layer combines with the normal layers (E, F_1, F_2) to produce characteristic types of echoes. These do not indicate fundamental differences in the layer itself for a particular zone. They do, however, support the conclusion that there is a fundamental difference between sporadic E of the auroral zone and that of the temperate zone. In discussing the mechanism of sporadic E, we shall only consider the thin layer type allowing that it may not be the explanation

of all features of the ionosphere which have at various times been identified as sporadic E.

The difficulty of explaining the sporadic-E layer in terms of the normal photochemical equilibrium of the ionosphere can best be illustrated by an example observed on the flight of Aerobee 4.48. The ionosonde at Wallops Island, operating at 5 minute intervals from 0600 showed a sporadic-E echo at each observation to the end of the 5 minute schedule one hour after the flight. During the rocket flight fE_s was 5.2 mc/s. The electron density profile, Figure 2-1, shows a sporadic-E layer with the peak at 102.9 km and a thickness of 3.0 km. From 8.8×10^4 cm^{-3} at 102.0 km, the electron density increases by a factor of 2.8 to 2.5×10^5 cm^{-3} at 102.9 km. If this were to be explained on the basis of the equilibrium equation

$$q = \alpha n^2 \qquad (2\text{-}1)$$

it would be necessary to postulate that, at the peak of the layer either (a) the rate of ionization, q, was increased or (b) the recombination coefficient, α, was decreased by the same factor of $(2.8)^2 = 8$ from what it was in the adjacent part of the E region. Either of these explanations is unacceptable and it is concluded that the sporadic-E layer is not formed in the same way as the normal ionospheric layers; a completely different mechanism must be invoked. Earlier attempts to explain the formation of sporadic E of the temperate zone by solar corpuscular radiation, meteor ionization and, in India, by thunderstorms have each been found to be inconsistent with observations.

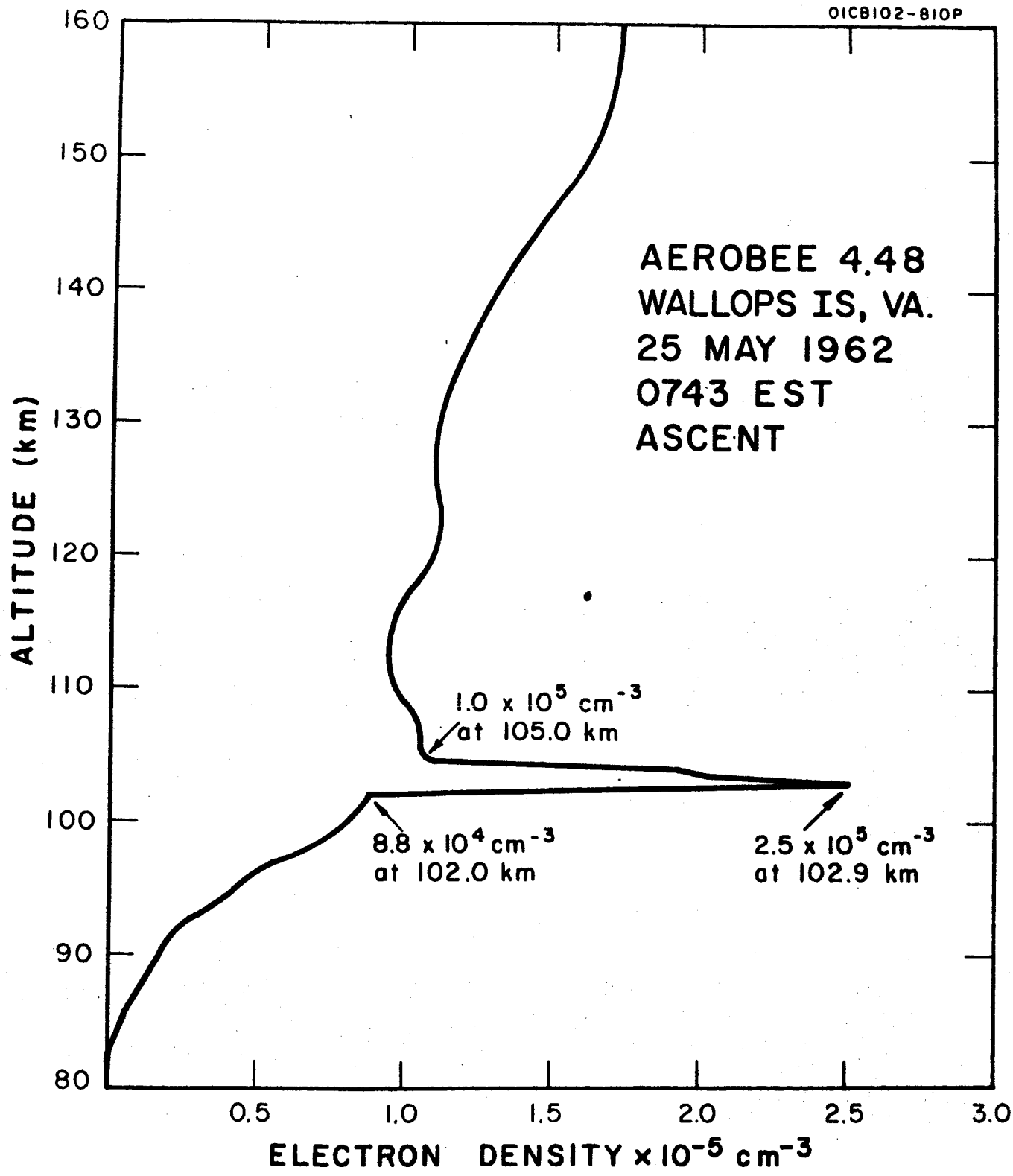

Figure 2-1. Electron density profile showing Sporadic E layer, 25 May 1962, 0743 EST.

The only acceptable explanation at present seems to be in terms of a redistribution of electrons from the normal E layer. Several authors have pointed out that horizontal motions of the atmosphere would, in the presence of the earth's magnetic field, impart a vertical velocity to the charged particles producing a vertical transport in the plasma. Whitehead[1-3] has deduced an expression for the vertical velocity V_z of ions; for the region below 120 km, where the ion collision frequency ν_i is greater than the ion gyrofrequency ω_{Hi} he finds that

$$V_z \approx \frac{\omega_{Hi} \cos \theta}{\nu_i} (U_y - \overline{U_y}) \qquad (2\text{-}2)$$

where θ is the magnetic dip-angle, U_y the E-W component of wind velocity and $\overline{U_y}$ the mean value of U_y in the region. Thus, in the presence of a wind shear ions will accumulate at the height at which $V_z = 0$. Since $V_z \propto \cos \theta$ this mechanism shows that the incidence of sporadic E should increase with the horizontal component of the earth's magnetic field. This is, in fact, supported by the observations in the temperate zone and is the strongest feature of the theory.

The existance of wind shears in the E region was first established through observations of long duration meteor trails and more recently systematic measurements have been made by introducing a man-made trail into the region. Up to the present time not enough data on wind structure is available to compare with the available statistics on sporadic-E occurrence. However, it does appear possible to use sounding rockets to examine a few specific cases of sporadic E to see if any obvious relation to wind shear existed. The three rocket flights of this project were therefore planned with this as the scientific objective.

SECTION 3

EXPERIMENTAL PROGRAM

3.1 PAYLOAD

The measuring technique for electron density is a variation of the Langmuir probe. In the normal Langmuir probe technique, an electrode is inserted into the plasma and the current to it measured as a function of the potential of the electrode. Analysis of the current-voltage curve gives electron temperature and electron density and, in the case of rocket and satellite applications, the vehicle potential. Since each sweep of voltage (a few volts negative to a few volts positive) gives only one value of electron density the technique is somewhat limited where rapid changes are occurring. This limitation has been overcome in the present instrument by keeping the electrode at a fixed (positive) potential for most of the time, interrupting this at regular intervals to sweep the potential in the manner of the normal Langmuir probe.[1-1] The current at fixed potential should be (and is) proportional to electron density. The only assumption made is that electron temperature is constant; the current is proportional to the average velocity of the electrons and hence varies as $(\text{temperature})^{1/2}$. Over the limited range of height in this investigation this appears to be a valid assumption. The proportionality of current to electron density has been verified in the flight of

Nike-Apache 14.31 which carried a DC probe (as we prefer to call the instrument) and a CW propagation experiment prepared by S. J. Bauer. With the arrangement we are using (nose tip electrode) the proportionality factor is such that an electron density of 10^5 cm^{-3} produces a probe current of 10 microamp for a probe potential of 2.7 volts.

Theoretically, the Langmuir probe is limited to a collision-free plasma which would limit its use to the ionosphere above about 90 km. However, on daytime flights we have measured probe current down to 50 km and the shape of the profile strongly suggests that the proportionality of probe current and electron density is maintained in the D region.

The payloads of Nike-Cajuns' 10.99, 10.108 and 10.109 are shown schematically in Figure 3-1. The major components and their functions are in sequence from the nose:

(1) Nose electrode. The nose tip of the payload is insulated from the body of the rocket and used as the electrode for the DC probe.

(2) Magnetic aspect sensors, Schonstedt Model RAM-3. Two aspect sensors are used, one mounted on the longitudinal axis of the rocket and used to measure the precessional motion and a second, transverse to the first, which is used to measure spin rate.

(3) Probe battery. Mercury cells are used to power the sweep circuit of the probe.

(4) Program unit. The electro-mechanical program unit generates the voltage waveform for the probe. It also introduces a periodic calibration and contains a commutator.

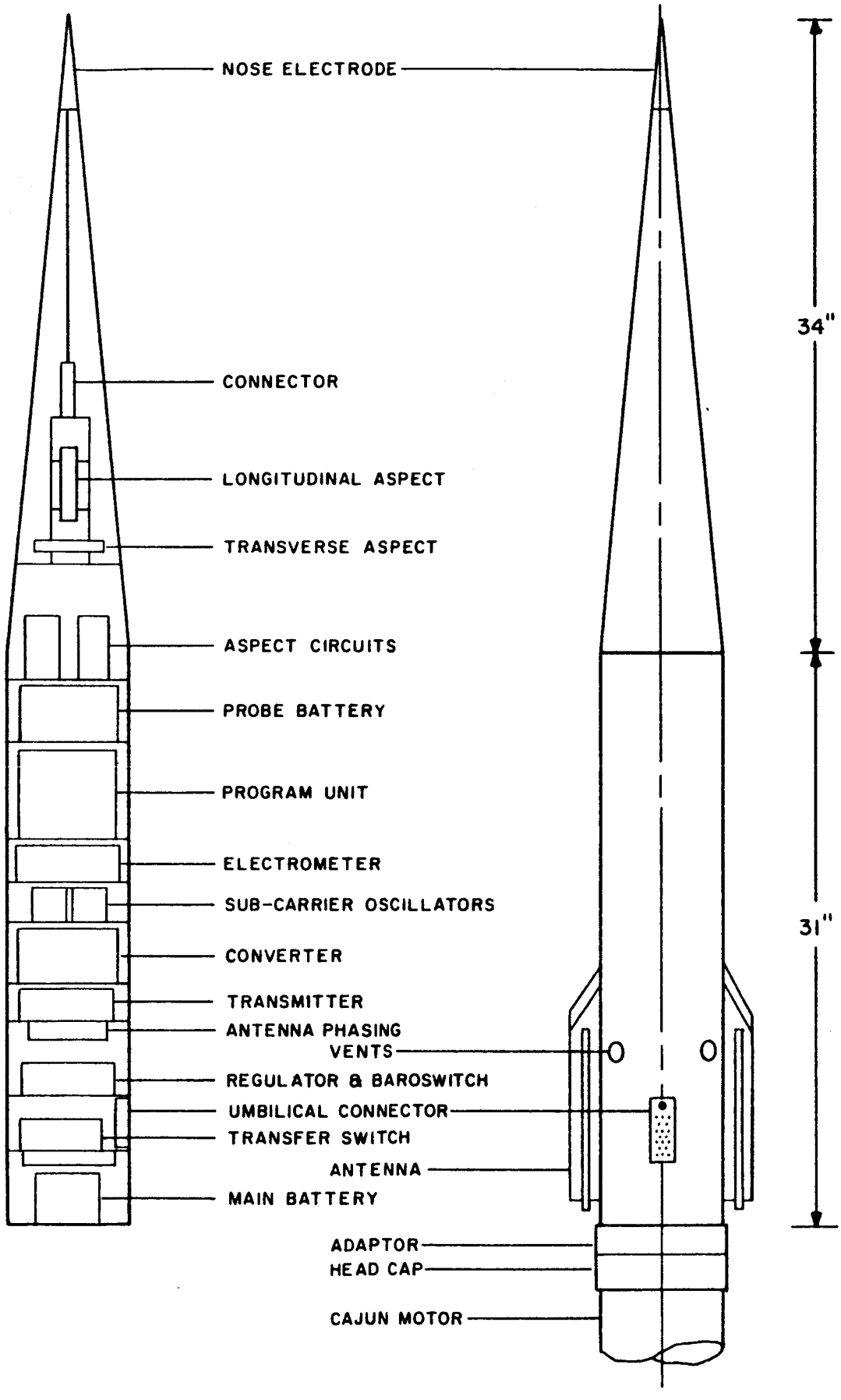

Figure 3-1. Payload configuration for Nike-Cajun 10.99, 10.108 and 10.109.

(5) Electrometer. A simple feedback electrometer is used to measure the probe current.

(6) Subcarrier oscillators, Data-Control Systems Model AOV-3S. Two S.C.O.'s are used: channel E (40 kc/sec ± 15%) carries the probe information and channel A (22 kc/sec ± 15%) the commutator output.

(7) Converter. The dc-to-dc converter generates + 200 v., + 6 v. and -28 v. for the electronic equipment.

(8) Transmitter, Telechrome Model 1475B. This FM/FM transmitter has a 2 watt output.

(9) Antennas. The two quadraloop antennas are fed in opposite phase.

(10) Regulator. This reduces the battery voltage to 28 ± 0.1 v.

(11) Baroswitch, Speidel Model AA200. These are used as altitude switches. Payload 10.99 carried two, one set for 55,000 ft and one for 70,000 ft. Payloads 10.108 and 10.109 carried one set for 55,000 ft.

(12) Umbilical Connector. A 20-pin connector is used, held by an explosive bolt (Holex No. 2503-10) which is fired from the blockhouse.

(13) Transfer switch. Power transfer (internal-external) is accomplished by a motor-driven bank of microswitches. Associated with this are two cut-off relays which remove all signals from the umbilical connector when de-energized.

(14) Battery, Eagle-Picher, No. 1025-V. This one-shot battery has an initial rating of 2 amp for 1 hour.

The overall length of the payload is 65 in and its weight is 53-1/2 pounds.

The probe calibration resistor was, on these three flights, connected through the baroswitch as shown in Figure 3-2. Thus a periodical calibration was obtained in the normal way prior to launch in the early part of the flight and at the end of the flight but this was replaced by a zero check during the major part of the flight. In practice the zero of the electrometer does not change appreciably after 30 minutes warm-up and the added complexity is not justified.

The arrangement of the commutator segments is shown in Figure 3-3.

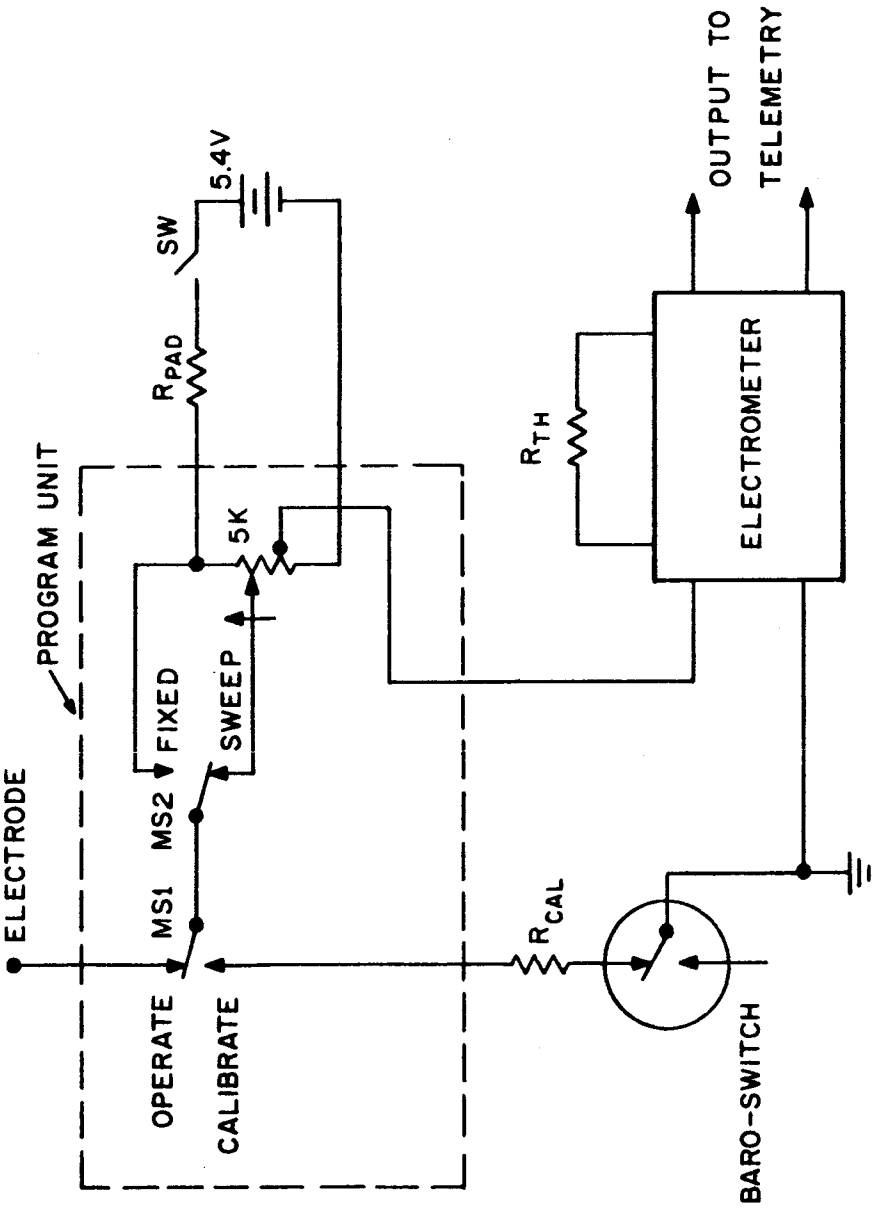

Figure 3-2. Langmuir Probe Circuit.

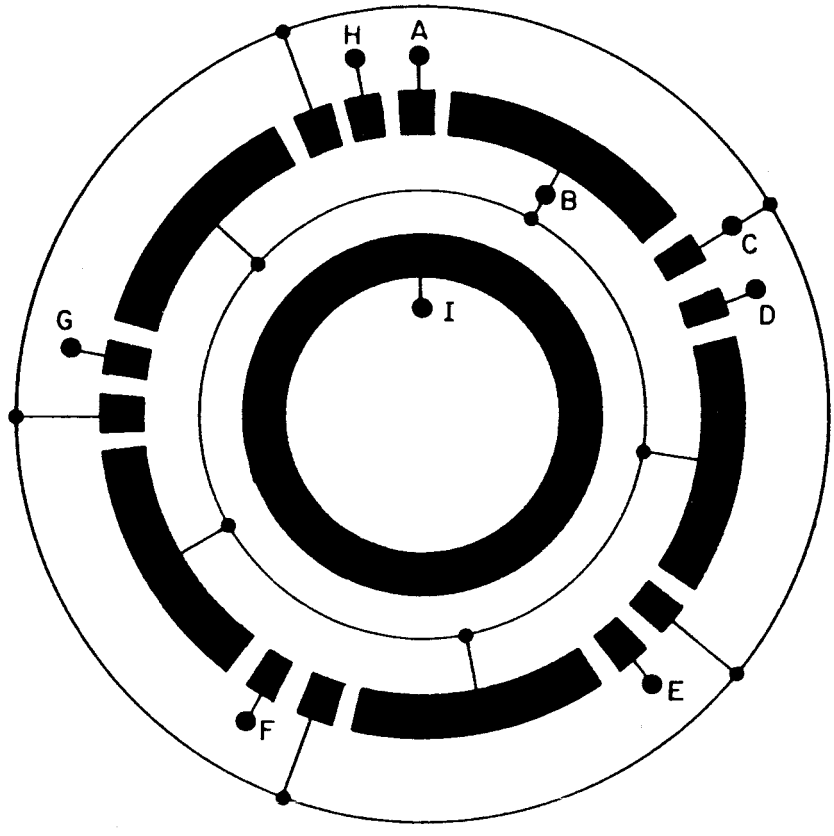

A: 5 volt (ref.)

B: Transverse Magnetometer

C: Longitudinal Magnetometer

D: Tr. Magnetometer Zero

E: Long. Magnetometer Zero

F: 0 volt (ref.)

G: Baroswitch 1 (55,000 ft)

H: Baroswitch 2 (70,000 ft)

I: Output

COMMUTATOR SEQUENCE: AHCBGCBFCBECBDCB
SEQUENCE DURATION: 0.5 second (nominal)

Figure 3-3. Commutator for Nike-Cajun 10.99, 10.108 and 10.109.

3.2 FLIGHT SUMMARY

The following information is given for reference.

(1) Nike-Cajun 10.99

Identification

Flight Number	:	NASA 10.99 CI
Wallops Model Number	:	G2-1092
Engine/Motor Number	:	1st Stage 19668, 2nd Stage PV-16-138-6
Rocket Type	:	Nike-Cajun
Number of Stages	:	Two
Place of Firing	:	Wallops Island, Virginia
Date of Firing	:	7 November 1962
Time of Firing	:	1025 Z; 0525 R

Flight Information (from Radar Skin Track)

		Predicted**	Observed
Peak Altitude:		93 st. mi.	81.5 st. mi.
Peak Time:		189 sec.	178 sec.
Ignition Data:	Time sec	Altitude ft	Velocity ft/sec
Bottom Stage	0	0	0
Stage 2	18.6	37,600	1510
Burnout Data:	Time sec	Altitude ft	Velocity ft/sec
Bottom Stage (est)	3.5	5600	3400
Stage 2	22.1	49190	5802

**Prediction based on flight weight - not estimated weight.

Impact Data:	Time sec	Impact Location	
		Range	Azimuth
Stage 2	354 sec	452,000 ft	104°

Launcher Setting:	Actual	Effective
Azimuth from True North:	100°	90°
Elevation above Horizontal:	77.5°	80°

Rocket Information

Total Rocket Measured Weight (including payload) 1594.6 lb.

(Propellant included in the above)

Total Rocket Length: 321.8 in.

Individual Stage Weights and c.g.'s:

	Weight lbs	C.G. in	C.G. Reference	Total Component Length (in)
Payload	53.5	46	Nose Tip	65.0
Stage 2	201			107.1
Stage 1	1340.1	75	N.E.P.	149.7
P.L. + Stage 2	254.5	65.5	N.E.P.	172.1

(2) Nike-Cajun 10.108

Identification

Flight Number : NASA 10.108 CI

Wallops Model Number : GZ-1093

Engine/Motor Number : 1st Stage 44038, 2nd Stage PV-16-138-10

Rocket Type : Nike-Cajun

Number of Stages : Two

Place of Firing	:	Wallops Island, Virginia
Date of Firing	:	30 November 1962
Time of Firing	:	1057 Z; 0557 R

Flight Information (from Radar Skin Track)

		Predicted**	Observed
Peak Altitude:		93 st. mi.	76 st. mi.
Peak Time:		189 sec	170 sec
Ignition Data:	Time sec	Altitude ft	Velocity ft/sec
Bottom Stage	0	0	0
Stage 2	20.8	39,400	1091
Burnout Data:	Time sec	Altitude ft	Velocity ft/sec
Bottom Stage (est)	3.5	5,600	3400
Stage 2	24.1	49,000	5423

**Prediction based on flight weight - not estimated weight.

Impact Data:	Time sec	Impact Location Range	Azimuth
Stage 2	346	69 st. mi.	96°

Launcher Setting:	Actual	Effective
Azimuth from True North:	117°	90°
Elevation above Horizontal:	83°	80°

Rocket Information

Total Rocket Measured Weight (including payload) 1594 lbs.

(Propellant included in the above)

Total Rocket Length: 321 in.

Individual Stage Weights and c. g.'s:

	Weight lbs	C.G. in	C.G. Reference	Total Component Length (in)
Payload	53.5	46	Nose Tip	65
Stage 1	1319.5	75	N.E.P.	150
Stage 2	201			107
P.L. + Stage 2	254.5	66	N.E.P.	172

(3) Nike-Cajun 10.109

Identification

Flight Number : NASA 10.109 CI

Wallops Model Number : G2-1094

Engine/Motor Number : 1st Stage 19707, 2nd Stage PV-16-138-12

Rocket Type : Nike-Cajun

Number of Stages : Two

Place of Firing : Wallops Island, Virginia

Date of Firing : 5 December 1962

Time of Firing : 2200 Z; 1700R

Flight Information*

		Predicted**	Observed
Peak Altitude		93 st. mi.	79.7 st. mi.
Peak Time		189 sec	178.1 sec
Ignition Data:	Time sec	Altitude ft	Velocity ft/sec
Stage 1	0	0	0
Stage 2	19.4	38,537	1373

Burnout Data:	Time sec	Altitude ft	Velocity ft/sec
Stage 1 (est)	3.5	5,600	3400
Stage 2	23.4	51,139	5593

Impact Data:	Time sec	Range n. mi.	Azimuth
Stage 1	---	---	-------
Stage 2	354.8	83.5	106.7°

Launcher Setting:	Actual	Effective
Azimuth from True North	93°	90°
Elevation above Horizontal	77.5°	80°

*Source: Radar Skin Track.

**Prediction based on flight weight - not estimated weight.

Rocket Information

Total Rocket Measured Weight (including payload) - NA

Total Rocket Measured C. G. (including payload) - NA

Individual Stage Weights and c. g.'s:

	Weight	C.G. in	C.G. Reference	Length
Payload	53.5	NA	-------	65
Stage 1	1,322.62	75 1/2	N.E.P.	151
Stage 2 (with payload)	255.5	65 1/2	N.E.P.	172.5

Times of stage ignition and burnout and loss of signal are given in Table 3-1. These are obtained from the telemetry record. There is a discrepancy in the time of second stage ignition of Nike Cajun 10.109 given in this table (T + 20.4 sec) and the value obtained from the tabulated radar data (T + 19.4 sec) and quoted in the flight summary. This rocket was launched manually, not by the automatic timer normally used, and it was noted at the time that the launch was almost one second before zero on the time count. It appears that zero time in the tabulated trajectory data is one second after the actual launch time. Such discrepancies as this could be avoided if the radar tabulation were expressed in Universal Time as are the time marks on the telemetry record.

TABLE 3-1

TIMES OBTAINED FROM TELEMETRY RECORD

10.99

1st Stage Ignition	1025:00.1 UT	(T)
1st Stage Burnout	1025:03.8 UT	(T + 3.7 sec)
2nd Stage Ignition	1025:18.8 UT	(T + 18.7 sec)
2nd Stage Burnout	1025:22.0 UT	(T + 21.9 sec)
Loss of TM (Splash)	1030:53.5 UT	(T + 353.4 sec)

10.108

1st Stage Ignition	1057:01.1 UT	(T)
1st Stage Burnout	1057:04.7 UT	(T + 3.6 sec)
2nd Stage Ignition	1057:21.9 UT	(T + 20.8 sec)
2nd Stage Burnout	1057:25.1 UT	(T + 24.0 sec)
Loss of TM (Splash)	1102:47.2 UT	(T + 346.1 sec)

10.109

1st Stage Ignition	2200:05.4 UT	(T)
1st Stage Burnout	2200:09.0 UT	(T + 3.6 sec)
2nd Stage Ignition	2200:25.8 UT	(T + 20.4 sec)
2nd Stage Burnout	2200:29.0 UT	(T + 23.6 sec)
Loss of TM (Splash)	2205:56.9 UT	(T + 351.5 sec)

3.3 VEHICLE PERFORMANCE

The performance of all three vehicles was rather lower than predicted: apogee altitudes of 131, 122 and 128 km were obtained compared with the predicted altitude of 149 km. Three earlier flights of a somewhat heavier payload with identical external configuration had given apogee altitudes of 153, 141 and 147 km, close to the predicted altitude. It is interesting to examine further the available data on the six flights to determine, if possible, the cause of the variation in performance.

Data relating to the performance of the second stage (Cajun) obtained from the radar tabulation is given in Table 3-2 for the six similar rockets. The time of second stage ignition together with the altitude and velocity at that time. The velocity increment of the second stage between ignition and burnout is also given as well as the maximum altitude attained. The predicted values appropriate to the last three flights are also given.

It is clear from the table that the second stage performance, judged by the velocity increment, is in all cases above predicted and cannot account for the low performance. The most obvious factor which points to the cause is the velocity at second stage ignition. All vehicles are lower than predicted and the last three more so than the first three. This low velocity could be caused by low performance of the first stage (Nike) or by unusually high drag during the coast between first stage burnout and second stage ignition. In view of the systematic

TABLE 3-2

SECOND STAGE PERFORMANCE (RADAR DATA)

Rocket	Ignition			Velocity Increment ft/sec	Maximum Altitude km
	Time sec	Altitude ft	Velocity ft/sec		
10.25	20.7	43,827	1593	4186	153
10.51	17.5	36,844	1701	4332	141
10.52	16.7	35,625	1761	4132	147
10.99	18.6	37,687	1511	4291	131
10.108	20.8	39,405	1091	4332	122
10.109	19.4*	38,537	1373	4219	128
Predicted	17.0	37,400	1820	4080	149

*The telemetry record indicates 20.4 sec.

nature of the degradation in performance and the fact that the proper burning time for the Nike was observed we are less inclined to suspect the Nike motor than the aerodynamics of the second stage.

The experience of this project shows the desirability of routinely measuring the performance of the first stage either by doppler radar at the launch pad or by an accellerometer on the vehicle. In either case much valuable information would be accumulated to give a better basis for vehicle design and trajectory prediction.

3.4 SPIN STABILIZATION

One of the objectives of the flights, unrelated to the primary objective, was an evaluation of spin stabilization for small sounding rockets. The spin was achieved by adding wedges to the trailing edge of the second stage fins and monitored by two aspect magnetometers.

The wedges on the first flight (10.99) were calculated to produce 5 rps. The magnetometers show that spin stabilization was not achieved and the payload executed a large precession cone. In the upper part of the trajectory the spin rate was 2.7 rps and the precession cone had a half-angle of 46° and a period of 54 sec. The spin rate in the early part of the flight could not be determined due to the temporary loss of signal from the magnetometers.

The wedges on the subsequent two flights were redesigned to produce 6 rps. The magnetometers show that spin stabilization was achieved, in both cases the included angle of the precession cone was 8.8°. The spin rate of 10.108 reached a peak of 6.8 rps at T + 30 sec and decreased to a constant rate of 5.4 rps in the upper part of the trajectory. Similarly 10.109 reached a peak of 7.7 rps at T + 25 sec which decreased to 4.6 rps in the upper part of the trajectory. The periods of the precession cones were slightly different: 40 sec for 10.108 and 44 sec for 10.109.

The experience of these flights was used as the basis for a subsequent series of Nike-Apache flights. Wedges were used to give a spin

rate of 6 rps. However, of seven rockets, two failed to spin up and executed large precession cones (14.87 and 14.88). The other five were successfully stabilized (14.86, 14.91, 14.92, 14.93 and 14.94) at the proper spin rate.

It appears, on the basis of experience with ten rocket flights, that there is a 30 percent probability that the wedges will be ineffective and that the second stage and payload will execute a large precession cone ("flat spin"). There is a 70 percent probability that stabilization will be achieved, the included angle of the precession cone being no greater than 10^{o}. In view of the importance of attitude stabilization, preferably at a rather lower spin rate, for many instruments carried by sounding rockets it is suggested that the problem should be attacked vigorously with theoretical studies, wind-tunnel tests and more test flights.

SECTION 4

OBSERVATIONS

4.1 ELECTRON DENSITY AND WIND STRUCTURE

The technique used by Manring and Bedinger in measuring the wind structure is to release a trail of sodium vapor as the rocket ascends and photograph the trail at intervals from four well-separated ground stations.[4-1] At present the technique is limited to periods near sunrise and sunset when the earth's shadow is at about 85 km. Of the series of three pairs of rocket shots at Wallops Island only the first could be held for occurrence of Sporadic-E as shown on the ionosonde. The sodium rocket must be launched close to a particular time so we set the launch time for the DC-4 probe rocket 30 minutes earlier and were prepared to "hold" for 20 minutes. The rocket carrying the probe could have been launched after the sodium rocket since it is unlikely that the sodium release would disturb the ionosphere, but it was felt that this might lead to some confusion with other rocket shots where the primary purpose has been to create an artificial ionosphere. We were prepared to try on successive days but fortunately the conditions were right on the first day and the electron density measurement preceded the wind measurement by 28 minutes.

The electron density profile is shown in Figure 4-1. The Sporadic E layer is about 4 km thick occurring between 98 and 102 km. The peak electron density was greater than anticipated; full scale deflection represents an electron density of 3×10^4 cm^{-3}. Beyond that point a clipping diode takes over and a very highly compressed scale results. The peak electron density in the layer, on descent, is actually about 1×10^5 cm^{-3}. The difference in layer structure on ascent and descent is interesting. The separation of the two penetrations is 67 km horizontally and about 3 min in time. The ascent shows a bifurcation of the layer with a peak density of a little over 3×10^4 cm^{-3} while on descent a single more intense layer is observed.

This profile also shows the rather irregular nature of the nighttime E region noted in previous observations.[1-2] An upper layer occurring between 119 and 123 km should also be noted. Above this layer the electron density falls off to 950 cm^{-3} at rocket apogee (131 km).

The wind structure is shown in Figure 4-2 in the form of two components, North-South and East-West, magnetic. The two layers are indicated. It is seen that contrary to expectation each is associated with an East-West shear in which the motion is toward the East below the layer and toward the West in and above the layer. Shears in the opposite sense, occurring at 91 and 111 km do not correspond with any significant feature of the electron density profile. The general motion within the layers is toward the North at about 40 m/sec for the main E_s layer and toward the South at about 70 m/sec for the upper layer. The boundary of the main layer seems to be defined by the North-South component.

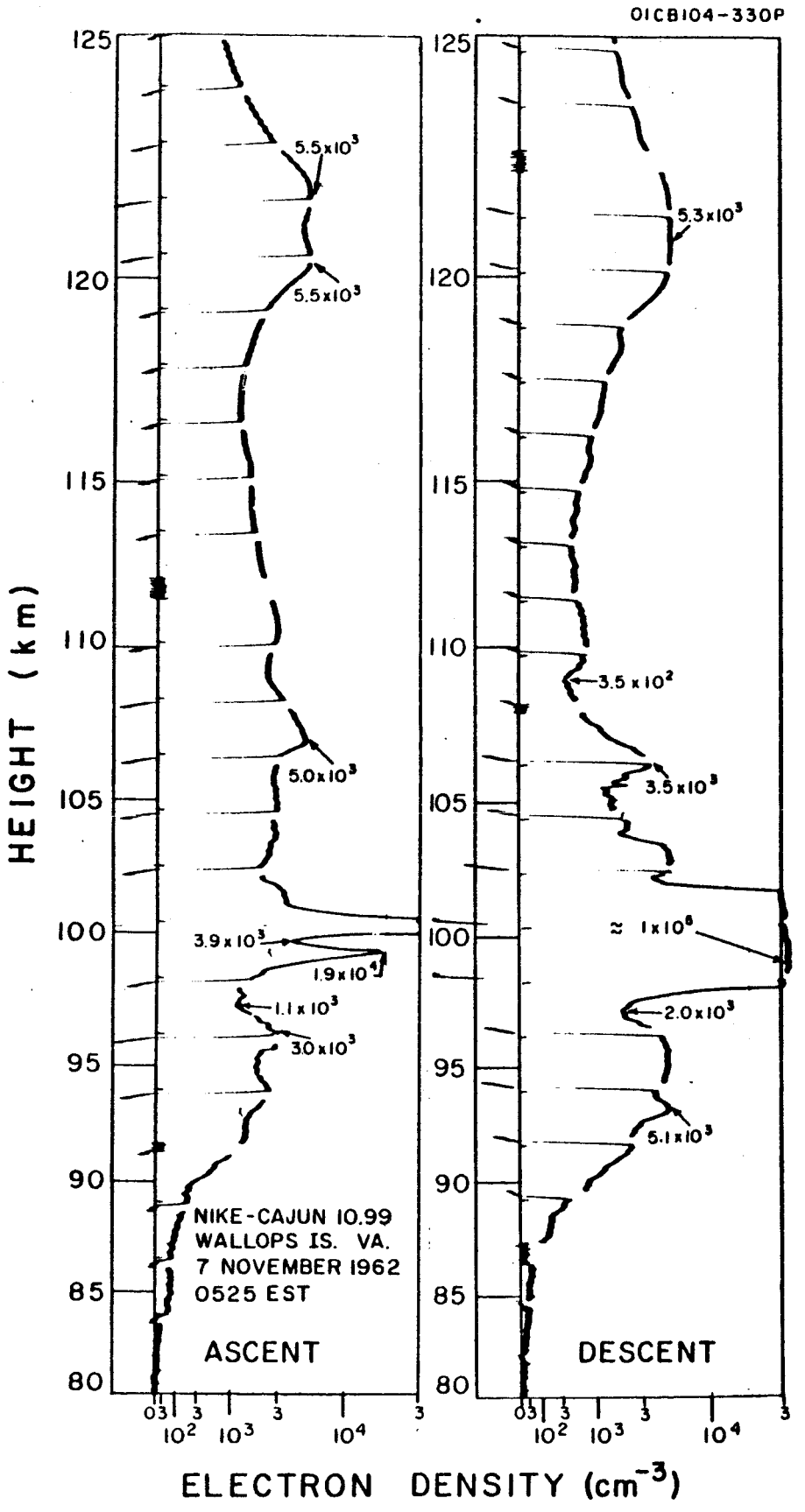

Figure 4-1. Electron density profiles, 7 November 1962, 0525 EST.

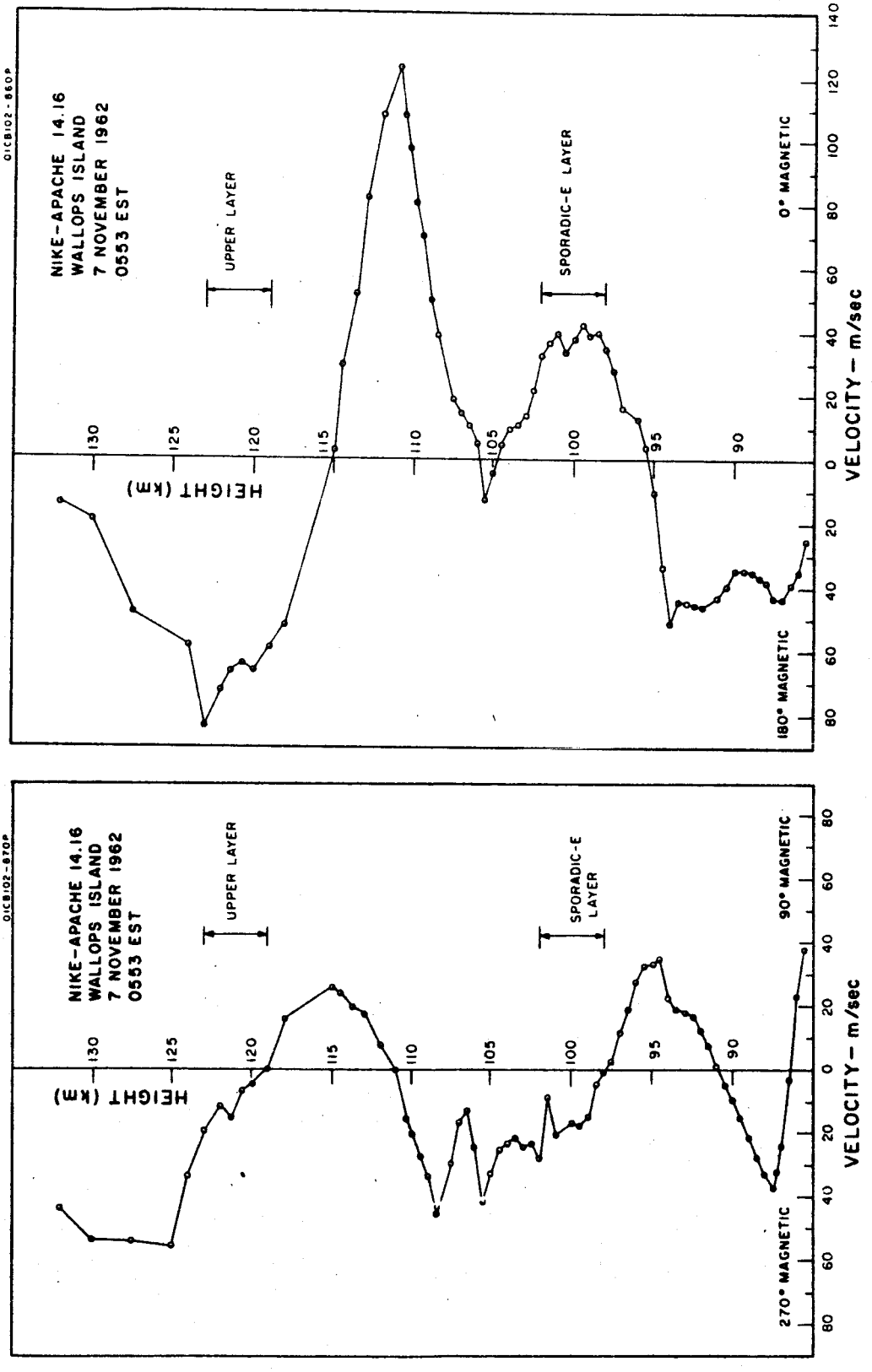

Figure 4-2. **Wind Components, 7 November 1962, 0553 EST.**

The next pair of flights were made, as it turned out, into a disturbed ionosphere. The F_2 critical frequency had dropped below 1.9 Mc/s and from 0459 to 0605 no value was recorded; the ionosonde record was in fact completely blank during the electron density flight launched at 0557. The electron density profile is shown in Figure 4-3. This pre-dawn profile differs noticeably from the previous nighttime observations in the scale of irregularity. The most prominent feature of the profile is a small peak at 100 km. It shows up both on ascent and descent (horizontal separation 47 km) and is regarded as a very weak sporadic E layer. Above 111 km the electron density decreases steadily to a value of 1.7×10^3 cm^{-3} at apogee (122 km) and is still decreasing.

The wind data recorded 18 minutes later, Figure 4-4 shows that the weak layer occurs in the same position relative to the East-West wind shear as had been noted on the previous flight. However, the previous flight had shown layers to be occurring near a maximum of the North-South component whereas this layer is located close to a minimum in the North-South component.

The third pair of flights were made at sunset. The electron density profile, Figure 4-5, shows the irregular structure characteristic of the nighttime E region. The horizontal separation of the profiles at 100 km altitude is 72 km. The lack of correspondence between the two profiles in the height range 108 to 118 km is unusual. The peak values of electron density on ascent and descent are about equal (9.4×10^4 cm^{-3} and 8.9×10^4 cm^{-3}) but the heights do not correspond. A similar lack of correspondence was found in the height range 101 to 107 km on an earlier flight (Nike-Cajun 10.52).

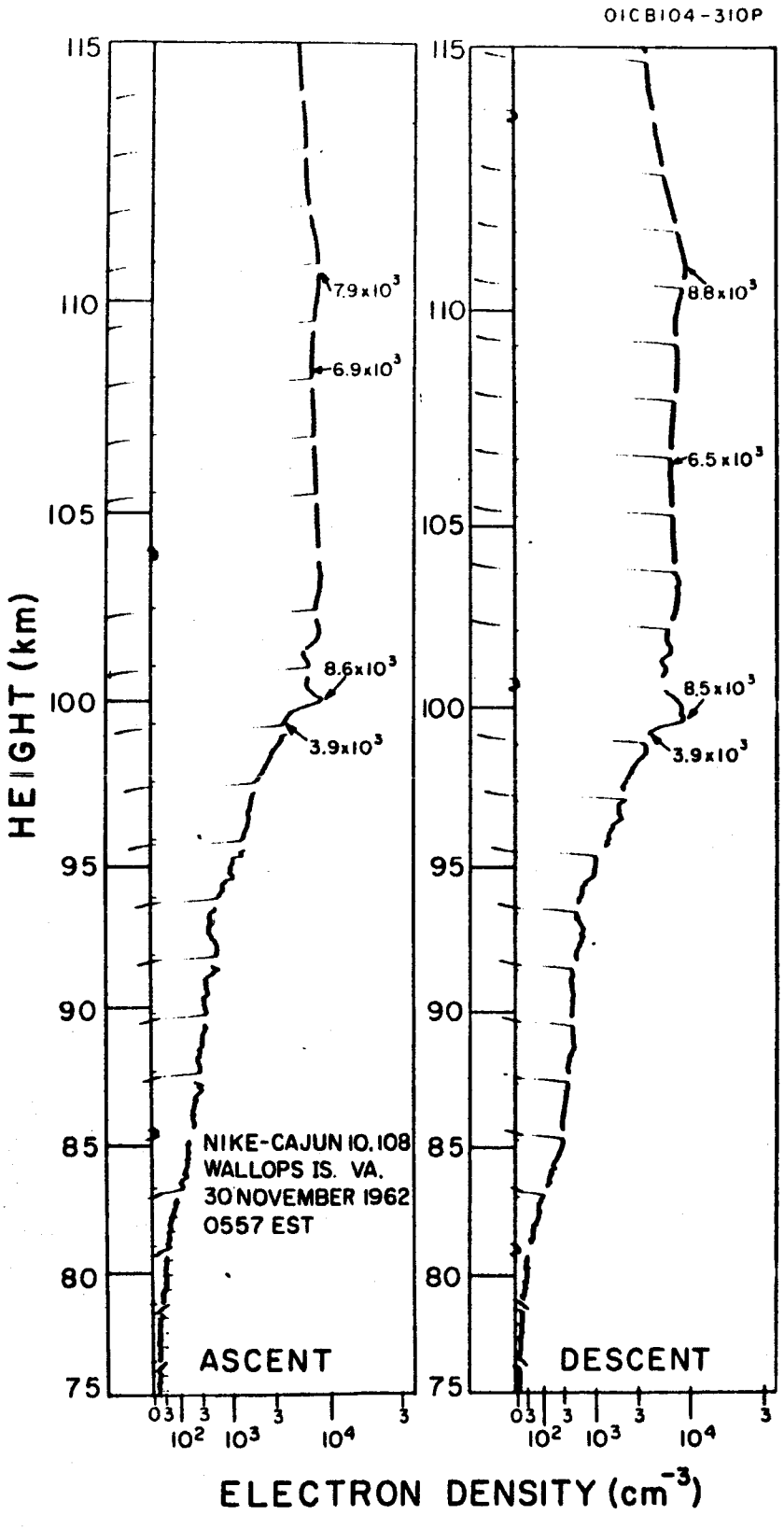

Figure 4-3. Electron density profiles, 30 November 1962, 0557 EST.

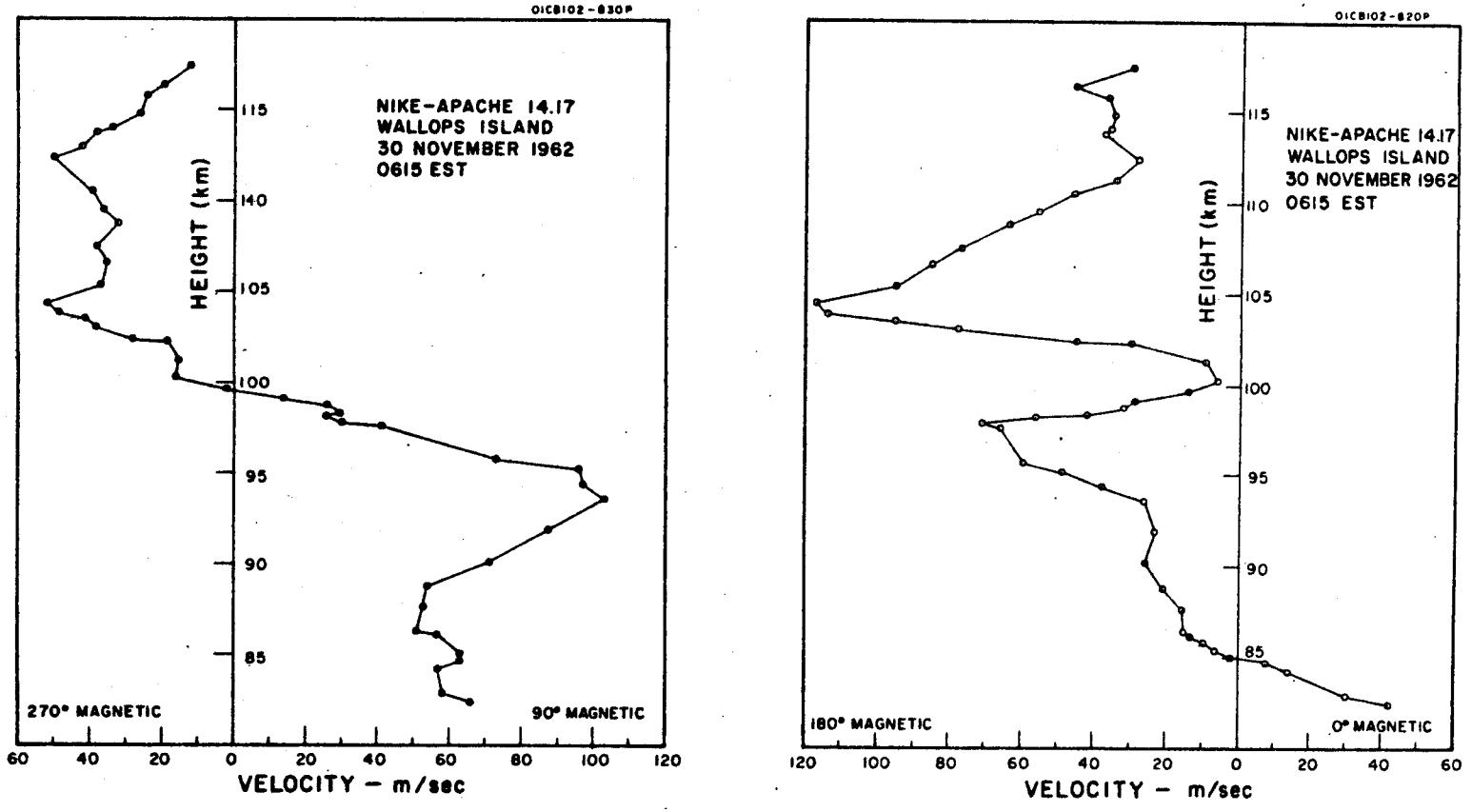

Figure 4-4. Wind Components, 30 November 1962, 0615 EST.

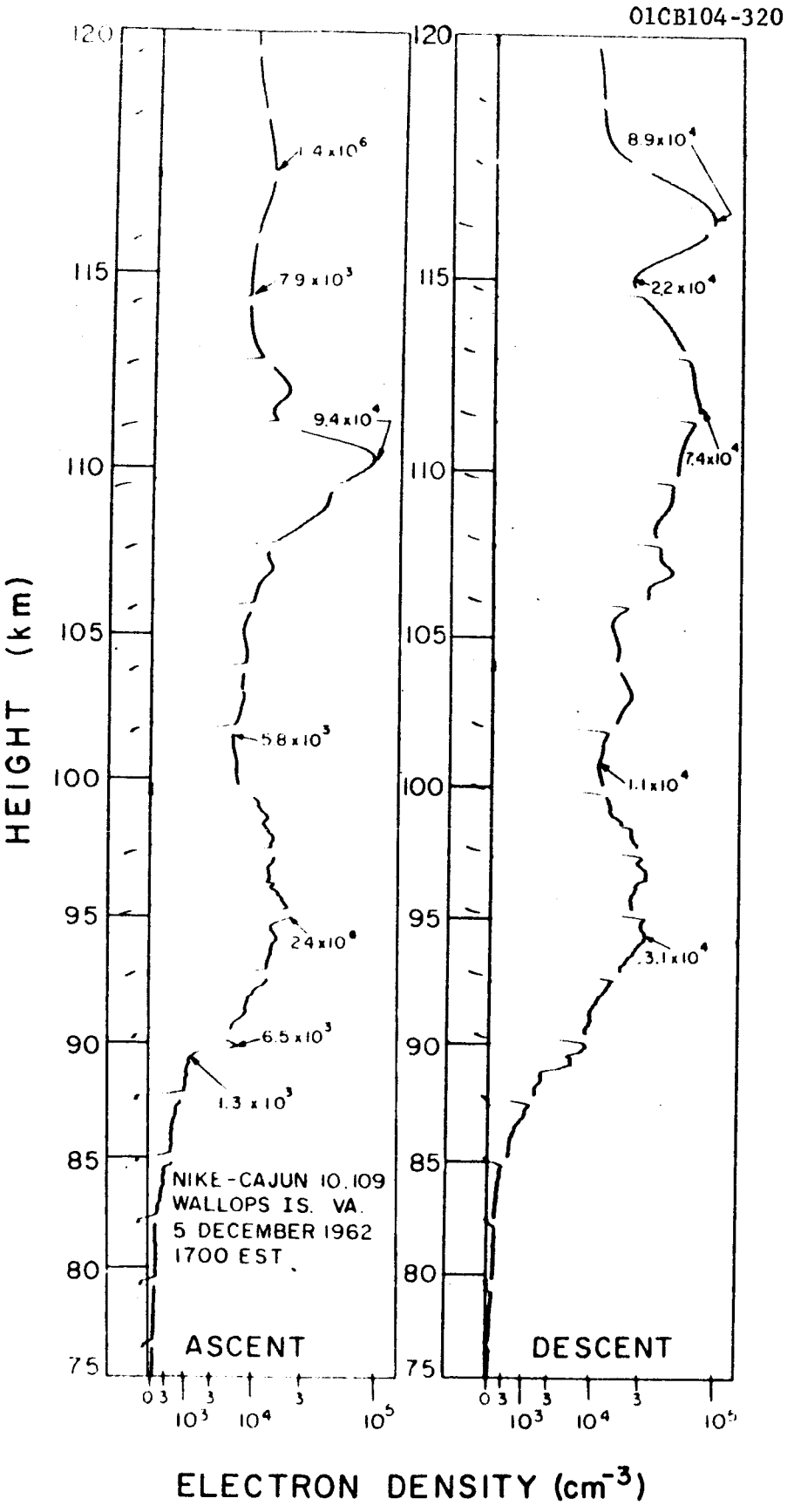

Figure 4-5. Electron density profiles, 5 December 1962, 1700 EST.

Sporadic E was recorded by the ionosonde during the flight with a maximum frequency fE_s ranging from 7.7 Mc/s to 9.6 Mc/s. The virtual height was recorded as 110 km. This agrees in height with the largest peak on the ascent profile but in view of the absence of a corresponding peak on the descent profile it is not established that this was the feature producing the sporadic E echo.

At rocket apogee (128 km) the electron density was found to be $6.3 \times 10^3 cm^{-3}$ which may be compared with a value of about $1 \times 10^3 cm^{-3}$ in the pre-dawn measurements and about $1 \times 10^5 cm^{-3}$ in daytime profiles.

The wind components, obtained 16 minutes later, are shown in Figure 4-6. Due to poor visibility parts of the profiles are missing (dashed lines). The East-West profile is unusual in that it does not show any shears crossing the axis. The features of the electron density profile, either ascent or descent, cannot be identified with features on the wind profile.

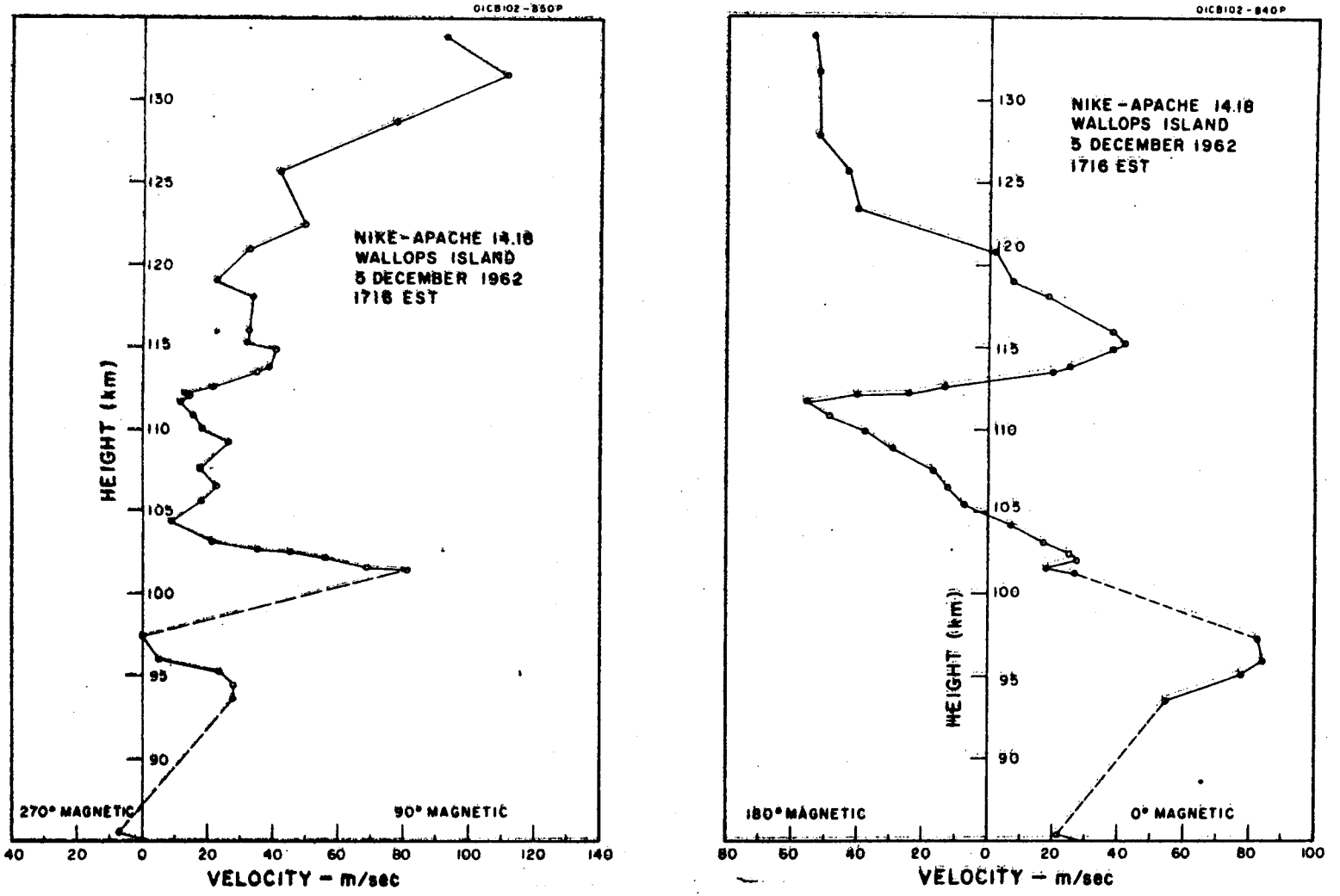

Figure 4-6. **Wind Components, 5 December 1962, 1716 EST.**

4.2 ELECTRON TEMPERATURE

The measurement of electron temperature in the nighttime E layer is limited to the height range 100 to 120 km. Below 100 km the validity of the Langmuir probe technique is doubtful while above 120 km the electron density falls off to low values and the measurement is inaccurate. The two pre-dawn flights (10.99 and 10.108) show a rather large range of values with no significant variation with height. Most values lie between 350^{o} and 550^{o}K with a probable error in each value of $\pm$ 50^{o}K. There are somewhat lower than values obtained on the previous pre-dawn measurement (Nike-Cajun 10.52) where the average was 580^{o}K with a range of $\pm$ 100^{o}K. It is interesting to note that the flight in the disturbed ionosphere (10.108) gave values of electron temperature not significantly different from those obtained in the quite ionosphere (10.99). Nor was the electron temperature in the sporadic-E layer different from that in the adjacent region of the nighttime E layer.

The measurement at sunset (10.109) showed a somewhat lower electron temperature in the height range 100-120 km. The average value is 300^{o}K with a range of $\pm$ 50^{o}K. A rapid rise of temperature occurs in about 2 km near 120 km altitude and from there to apogee (128 km) the average electrom temperature is 450^{o}K with a range of $\pm$ 50^{o}K.

The measurements obtained to the present do not indicate any pattern to the measurements of electron temperature but neither does the electron density structure of the nighttime E layer show a regularity

from night to night. There is a need for more data on both electron temperature so that a search can be made for regular variations, (with season, solar cycle, etc) and irregular variations (during ionospheric storms, for example or periods of high meteor activity).

The measurements so far have always indicated a maxwellian energy distribution i.e., thermal equilibrium among the electrons, at least up to an energy several times greater than the mean energy. It is felt that this can be assumed to be true in future (routine) measurements and the very tedious analysis of the current-voltage curve avoided. Several methods are available generally involving small audio frequency signals superimposed on the linear voltage sweep.[4-2] The electronic circuits are not difficult to develop and can be incorporated in the airborne instrument. This approach has the additional advantage that electron temperature may be transmitted as an analog voltage at a greatly reduced bandwidth.

4.3 MEASUREMENTS IN THE D REGION.

The interpretation of the probe data in the D region (50-90 km) is not entirely clear. The Langmuir probe technique is not strictly valid below 90 km for two reasons: (a) the presence of nagative ions cannot be ignored and (b) the mean free path of the electrons becomes small compared with the Debye length. In the D region it would appear that the current flowing into the electrode is determined by the polar conductivity of the surrounding medium and, in the actual case of the floating bipolar probe in the ionosphere, the current in the system is determined by the lower of the two polar conductivities i.e., by the component of conductivity due to positive ions. The data from an earlier flight (Nike-Cajun 10.25) was analyzed on this basis and gave an acceptable profile of positive ion density.(4-3)

Daytime measurements of probe current begin at about 50 km while at night, with somewhat increased sensitivity, current is first measured at about 75 km. Now very little is known with certainty about the lower D region (below 70 km) but it is believed that the ionization (under quiet solar conditions) below 70 km is due only to cosmic rays. Thus the positive ion density should not show any marked diurnal variation and the positive ion conductivity should not change significantly from day to night. It appears, even without detailed theoretical analysis, that the probe current cannot be satisfactorily explained in terms of the conductivity measurement.

An acceptable interpretation of the data is, however, obtained if it is assumed that the proportionality of probe current with electron density established in the E region also holds true in the D region. It has not yet proved possible to check the DC probe against an independent measurement of electron density in the D region. However, we feel it gives a significant picture of the structure of the region although the actual values of electron density obtained this way should be treated with caution.

The profiles of probe current obtained from the flights of Nike-Cajuns 10.99, 10.108 and 10.109 are shown in Figure 4-7 together with a subsequent daytime profile. The probe current was measured at a potential of + 2.7 v. and,for clarity, only ascent data is plotted; on descent through the region the profiles were retraced with no significant differences.

The daytime profile shows clearly the so-called C layer between 50 and 65 km with the peak at 58 km. The D layer, between 65 and 82 km, corresponds with the absorption of Lyman-α radiation. Above 82 km the electron density increases smoothly into the E layer.

The two pre-dawn profiles (10.99 and 10.108) show the steeper gradient typical of the region at night. The profile at sunset (10.109) is most interesting. The electron density in the D region is reduced by about an order of magnitude below the daytime values; the exception is the valley between 58 and 70 km but on other occasions this valley has been much less pronounced. At sunset no ionizing radiation except cosmic rays reach the atmosphere below 90 km and it might be expected that the nighttime conditions

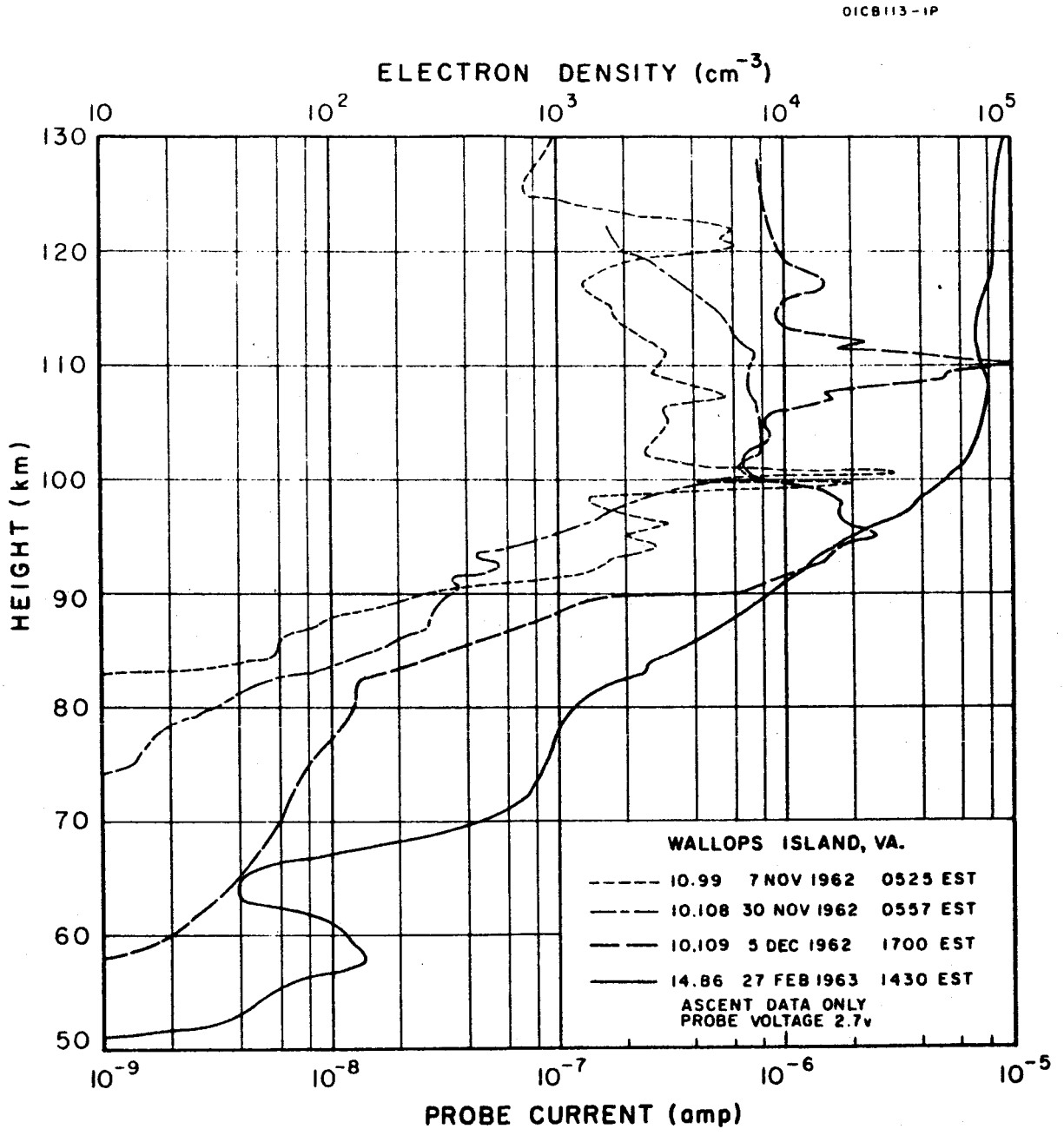

Figure 4-7. Profiles of probe current in the D and lower E region.

would already be established. The only possible explanation consistent with current ideas of the formation of the D region is that it is due to photodetachment of electrons from ionization produced by cosmic rays. The solar radiation penetrating to this region is in the near UV (responsible for the ozone layer near 30 km), the visible and infrared part of the solar spectrum. Further measurements designed to examine the transition at sunset from day to night conditions as the sun's shadow rises would do much toward an understanding of the D region. Systematic measurement of the changes in the D region profile near sunset and similarly near sunrise promises to be a powerful method of studying the processes determining the structure of the region.

SECTION 5

CONCLUSIONS AND RECOMMENDATIONS

Two features characterize the structure of the nighttime E region. The first is the deep trough which separates the E and F layers at night. The lower boundary of this trough occurs at about 125 km. By dawn the electron density in this region has fallen to several hundred per cm^3.

The second feature is the general irregularity of the nighttime E layer. Its variability from one night to another is in marked contrast to the regular behaviour of the daytime E layer.

The electron density profile obtained at sunset also shows irregular structure characteristic of the nighttime profiles. This was quite unexpected and indicates that a rapid change in structure occurs in the late afternoon.

In view of the generally irregular nature of the region at night and the marked stratification the identification of Sporadic E layers is more difficult than in the daytime profiles. However, the height of occurrence is most often within a few kilometers of 100 km. The

three most intense cases we have observed have peaks at 102.5 km (Nike-Cajun 10.51, night), 102.9 km (Aerobee 4.48, day) and 99.5km, (Nike-Cajun 10.99, night). Seddon[5-1] has reported cases with peaks at 100.9 km (Aerobee NRL-50, day) and 98 km (Aerobee NN3.11F, night) and quotes a nighttime observation of H. S. W. Massey showing a peak at 100.5 km. This narrow range of height (98-103 km) distinguishes Sporadic E from the less pronounced ledges and layers which are commonly found on the electron density profile up to 90 km in the day and up to 120 km at night.

Comparison of the electron density profiles with the wind observations has indicated a definite relation in layer formation. The particular feature of the wind profile is a shear in the East-West component in which the motion is towards the East on the low side and toward the West on the high side. Three examples of this type of shear (above 90 km) each gave rise to a layer. On the flight of 7 November 1962 such a shear at 98 km produced an intense Sporadic E layer while a comparable shear at 119 km produced a rather weaker layer. On the flight of 30 November 1962 the shear at 99.5 km produced a minor layer. No shear of this type was observed on the flight of 5 December 1962, nor did the electron density profile contain a clearly identifyable Sporadic E layer. However the ionosonde was indicating strong Sporadic E. This must be regarded as an anomalous case neither supporting nor disproving the relation which was indicated in the previous measurements.

It is interesting that each of the three layers is centered somewhat above the point of zero velocity indicating a net motion to the West. This combines with the North-South component to determine the actual motion of the layers.

The role of the North-South component of wind is not clear. In the case of the intense sporadic-E layer of 7 November 1962 it appears to define the boundaries of the layer.

The observations support Whitehead's theory of the formation of the sporadic-E layer. There are two features, however, which the theory does not explain. The first concerns the height of occurrence. It has been noted that the layer is most frequently observed to occur at an altitude close to 100 km. This may be interpreted to mean that the particular wind shear also has a strong preference for this height or, and this is felt to be more feasible, some factor has been omitted from the theory which produces a "resonance" effect at this height.

The second feature which is not adequately explained by the Whitehead theory is the source of the ionization in the layers. If it is transported from adjacent regions there should be a noticable reduction in electron density in the normal E layer. This would show up clearly in the daytime measurements but, apparently, the E layer peak electron density (as shown by the critical frequency) is not reduced when sporadic E forms.

The simple experimental techniques used in this project have established the feasibility of direct measurement of sporadic E and have indicated a definite relationship with winds. Further measurements, more nearly simultaneous, are required to difinitely establish this relationship and to determine what other features, if any, of the electron density profile are related to wind structure.

REFERENCES

1-1 Smith, L. G., "A DC Probe for Rocket Measurements in the Ionosphere," GCA Technical Report No. 63-19-N, (June 1963).

1-2 Smith, L. G., "Rocket Measurements of Electron Density and Temperature in the Nighttime Ionosphere," GCA Technical Report No. 62-1-N, (January 1962).

2-1 Harwood, J., "Some Observations of the Occurrence and Movement of Sporadic-E Ionization," J. Atmos. Ter. Phys., 20, 243-262, 1961.

4-1 Jenkins, R. J., and E. R. Manring, "The Design, Construction and Operation of Ground-Based Tracking Equipment for Experiments Utilizing Optical Trace Materials to Study Atmospheric Parameters," GCA Technical Report No. 61-2-N, (March 1961).

4-2 Branner, G. R., E. M. Frair and G. Medicus, "Automatic Plotting Device for the Second Derivative of Langmuir Probe Curves," Rev. Sci. Inst., 34, 231-237, 1963.

4-3 Smith, L. G., "Electron Density in the Ionosphere," GCA Technical Report No. 63-23-N, (July 1963).

5-1 Seddon, J. C., "Sporadic E as Observed with Rockets," NASA Technical Note D-1043, (July 1961).

APPENDIX A

A SIMPLE METHOD OF TRAJECTORY DETERMINATION FOR SOUNDING ROCKETS

This study of a simple method of trajectory determination for sounding rockets was generated by practical necessity. Six rockets (Nike-Apache) instrumented to measure electron density and solar radiation are to be launched from Fort Churchill during the eclipse of 20 July 1963. It is particularly important that an accurate trajectory be recorded for each flight so that the change in the electron density profile may be accurately observed. Radar tracking of the vehicles will be used but it was felt very desirable to provide an independant method of obtaining the vehicle altitude as a function of time; range and azimuth are less important for this and many other experiments. Dovap[A-1] and similar systems provide such an alternative technique but at the expense of added complexity in the payload and the ground station. Another approach in which the peak altitude is estimated from the time of flight from launch to impact has been shown to be useful.[A-2] The termination of the telemetry signal is not entirely satisfaction as a criterion of impact; the signal may be lost prior to impact under unfavorable conditions. The method also involves somewhat elaborate calculations of drag. In this note it is shown that a much simpler method is provided by using the time-of-flight above some reference altitude,

detected by an on-board device. When this altitude is made as high as possible (70,000 feet appears to be a practical limit) the correction drag becomes very small and the trajectory is determined with a minimum of computation. An altitude switch has been found to be a convenient method of marking the passage through the reference altitude; it is reliable and accurate, uses no power and is small in size and weight.

The evaluation of the technique has been made with respect to a series of five Nike-Cajuns launched from Wallops Island, Virginia, in the course of an investigation of the ionosphere using the Langmuir probe technique.* The payload weight varied between 53 and 58 lbs. but the external configuration was identical. It consisted of a cylindrical section 31 in. long, 6.5 in. diameter surmounted by an 11 degree nose cone, 34 in. long. Two quadraloop antennas were mounted externally on each payload. Three payloads (10.99, 10.108 and 10.109) carried altitude switches set for 55,000 feet, and in addition payload 10.99 carried an altitude switch set for 70,000 feet. The payloads were vented through four holes, 0.75 in. diameter, equally spaced on the circumference at 54 in from the nose tip. The altitude switches were Model AA200** manufactured by Speidel Corporation, Warwick, Rhode Island. The dimensions are: height 1.2 in., diameter 1.6 in., weight 2 oz. The unit cost is about $40. The units were individually recalibrated

---

* Under contracts Nos. NASw-98 and NASw-489.

** as received, they were labelled: No. 74-6617-F.

in a small altitude chamber and found to be very stable. Other altitude switches are available but it was beyond the scope of the project to evaluate other types.

The data obtained from radar for the five flights are given in Table A-1. The peak altitude is corrected for earth curvature, i.e. it is the actual height at apogee measured from sea level. The same data is represented graphically in Figure A-1 together with a theoretical free-fall curve (part of a parabola) where an effective value of the acceleration due to gravity (g') is chosen to give the best fit. It is seen that the limit of scatter of the points about this line is about $\pm$ 0.5 km. The low value of g' is not entirely accounted for by the decrease of g with height and must be regarded as an empirical value.

TABLE A-1

Time of Flight Above Reference Level

Rocket	55,000 ft	70,000 ft	Peak Altitude
10.51	325.8* sec	319.6* sec	141* km
10.52	334.1+ sec	328.1+ sec	147.1+ km
10.99	313.3+ sec	307.1+ sec	131.4+ km
10.108	300.0+ sec	293.2+ sec	122.0+ km
10.109	309.5+ sec	303.0+ sec	128.3+ km

*Radar, plot board data

+Radar, tabulated data

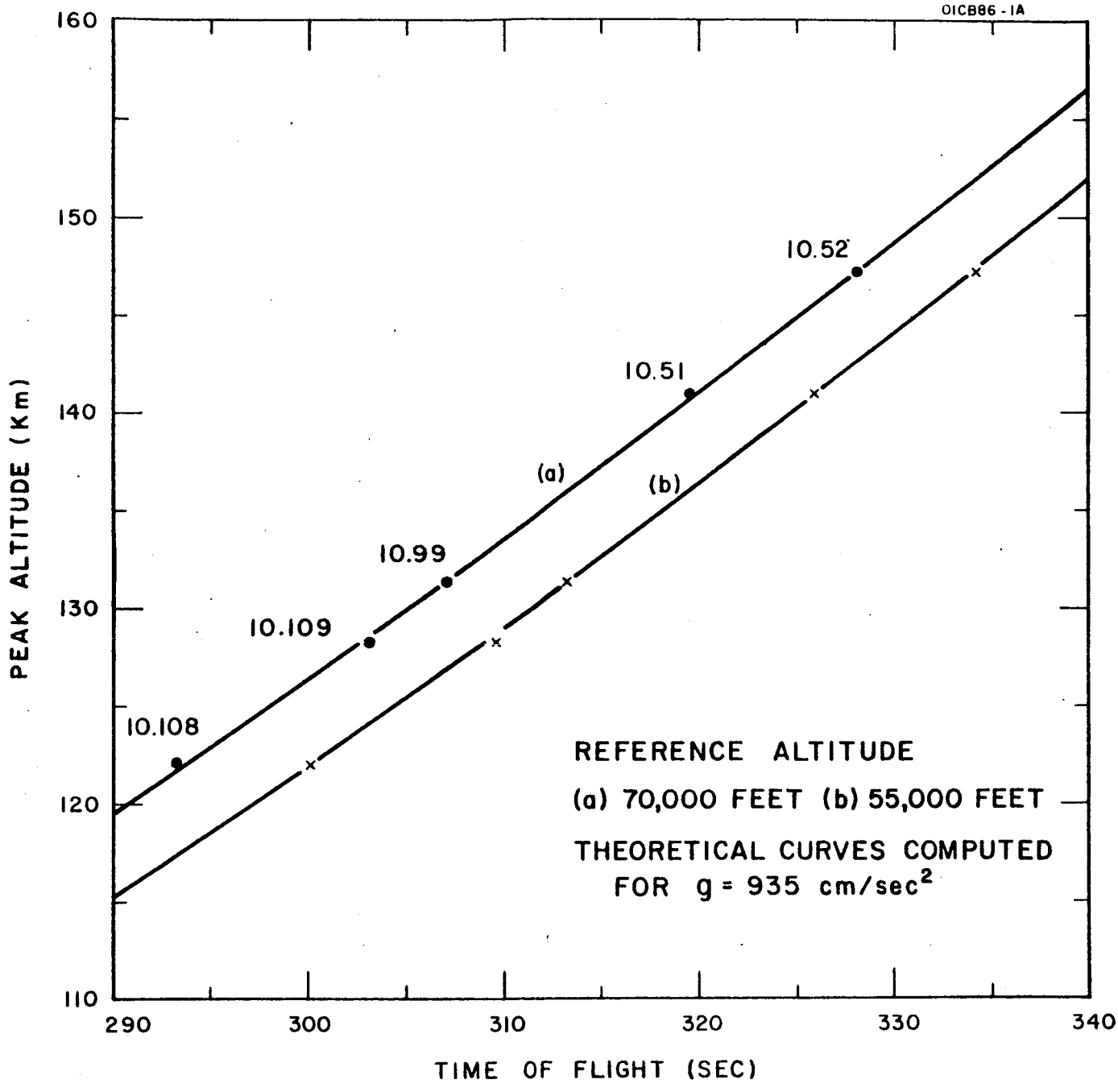

Figure A-1. **Time of flight above reference altitude.**

The technique may be understood by reference to Figure A-2 which shows the variation of the vertical component of velocity during the flight of a typical Nike-Cajun having a low-drag configuration. The data is obtained from the radar trajectory for this flight. The linear portion of this graph is the free-fall region and shows an effective value of g of about 940cm/sec^2. The initial and final portions (altitudes below about 125,000 feet) show the effect of aerodynamic drag. It is apparent, however, that above 70,000 feet the effect of drag is small.

The asymmetrial nature of the drag produces an asymmetry in the trajectory. This is illustrated in Figure A-3 in an exaggerated form. The parabola which coincides with the upper part of the actual trajectory crosses the reference altitude z_o at times t_1' and t_2' which are earlier than the actual times t_1 and t_2. In the case of Nike-Cajun 10.99, the actual trajectory shows that for a reference altitude of 70,000 feet t_1 and t_2 are 26.0 and 333.1 seconds after launch. The best-fit parabola leads to values of t_1' and t_2' which are both earlier than the observed values by 0.7 seconds. Similarly, for Nike-Cajun 10.52, the time difference $t_1 - t_1' = t_2 - t_2' = 0.4$ seconds. These times represent small corrections to the trajectory and the difference is not really significant. This leads to the empirical rule that an improved trajectory

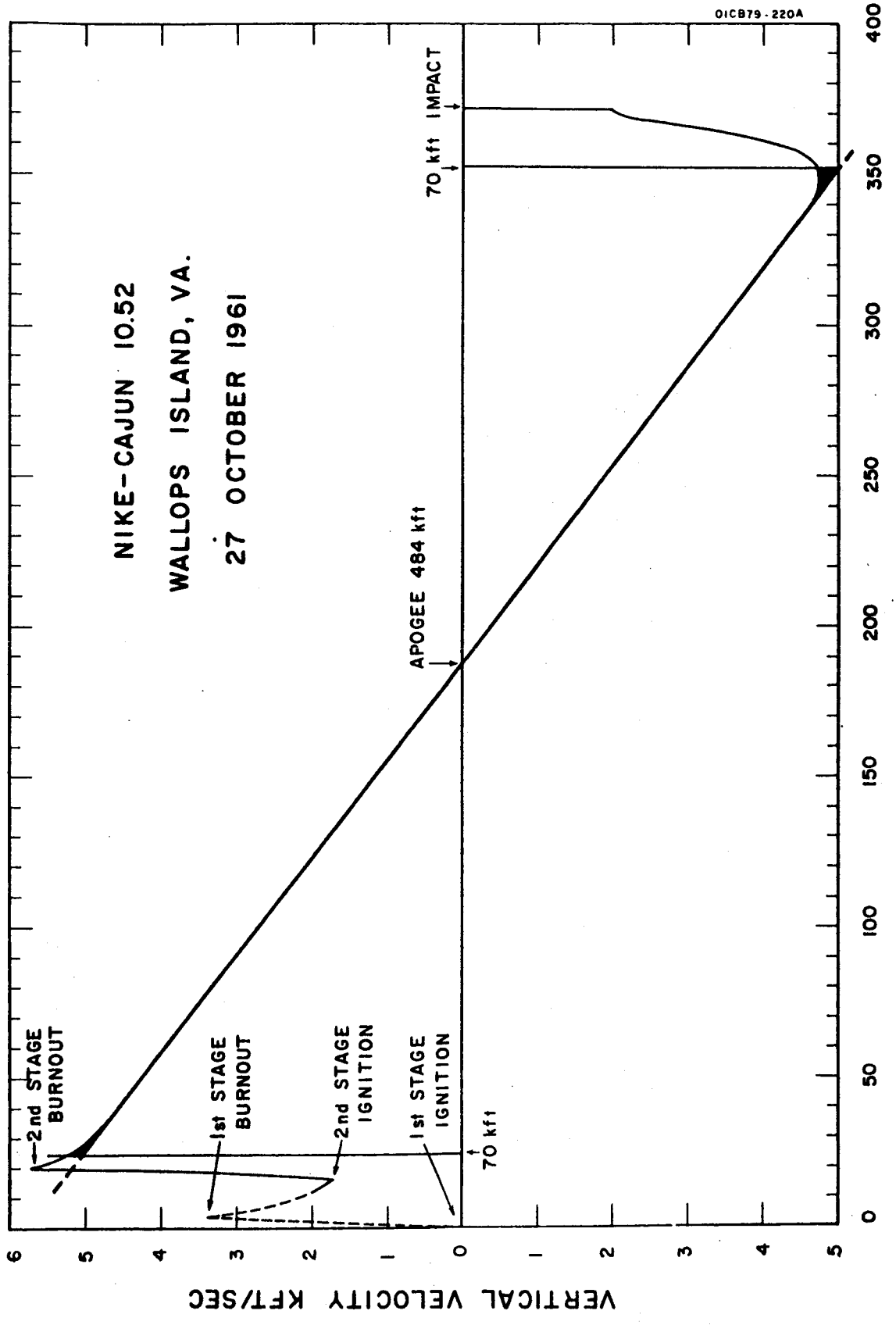

Figure A-2. Vertical component of velocity, Nike-Cajun 10.52.

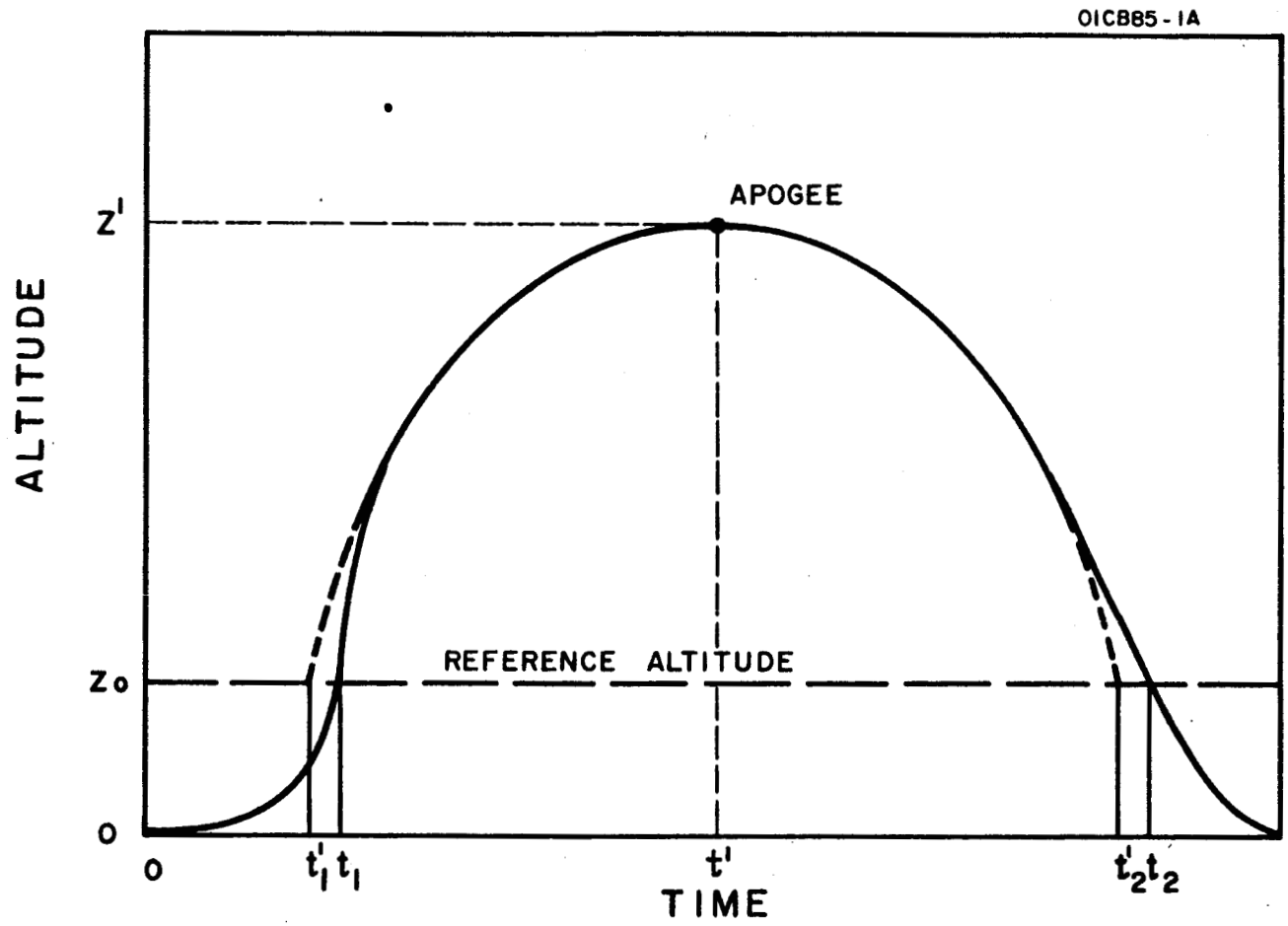

Figure A-3. **Effect of drag on trajectory, (exaggerated).**

is obtained by subtracting 0.5 seconds from the times at which the rocket passes the 70,000 feet reference altitude. This also implies that the actual time at apogee is earlier, by 0.5 seconds, than the mean of t_1 and t_2.

The equation of the trajectory (altitude versus time) may be conviently expressed by the following:

$$z = z' - \frac{1}{2} g' (t - t')^2$$

where z is the altitude above sea level at time t, z' is the altitude at apogee, g' is the "effective" value of g, and t' is the actual time of apogee, obtained from t_1 and t_2 as described above. The value of g' to be used in this formula includes an empirical correction for drag. It is determined by analysis of an actual trajectory. For the reference altitude of 70,000 feet, the best value of g' is found to be 936 cm/sec^2 for Nike-Cajun 10.52 and 933 cm/sec^2 for Nike-Cajun 10.99. Again, the difference is not significant and a mean value of g' of 935 cm/sec^2 is to be used for the series.

The time of flight above a reference altitude has been found to be a useful guide to the relative performance of a series of sounding rockets having similar payloads. It is also found that a small empirical correction can be applied and an accurate trajectory computed knowing only the times at which the rocket passes the reference altitude on ascent and descent.

The technique is potentially most valuable when a series of similar payloads is to be launched by the same type of vehicle in a large scale program such as is envisioned for the IQSY. The accurate tracking by radar at one site would serve as a basis for determining the trajectories of rockets at other sites not having tracking equipment.

REFERENCES

A-1. H. W. Zancanata "Ballistic instrumentation and summary of instrumentation results for the IGY rocket project at Fort Churchill", BRL Report No. 1091, January 1960.

A-2. C. T. Force "Estimation of sounding rocket trajectories from total time of flight," ARS J. 32, 1095-1097, 1962.

APPENDIX B

CALCULATION OF TRAJECTORY

The baroswitches, nominally set for 70,000 ft, are individually calibrated for decreasing pressure (ascent) and increasing pressure (descent). Due to the differential travel in the microswitch these two readings differ by an amount equivalent to about 1 or 2 km in altitude and, in practice, neither is exactly at the nominal setting of the baroswitch. The first step in computing the trajectory is to correct the observed switching times to the reference altitude of 70,000 ft (21.3 km).

The procedure for correcting the baroswitch and computing the apogee altitude and time is illustrated in Table B-1 by the data from Nike-Apache 14.92. Lines 1 to 4 identify the flight. Line 5 gives the values of the constants g' and z_o. Line 6 gives the baroswitch calibration determined prior to the flight. Line 7 gives the corresponding altitudes obtained from the 1959 ARDC Model Atmosphere. Line 8 gives the actual times of switching observed during the flight. The difference between these, (t_2-t_1), gives the time of flight uncorrected for the baroswitch altitude error. This first approximation to the time of flight

TABLE B-1

COMPUTATION OF APOGEE ALTITUDE AND TIME

1. Rocket: Nike-Apache 14.92
2. Date: 20 July 1963
3. Time: 2113:00 UT
4. Place: Fort Churchill, Manitoba
5. Constants used: $g' = 935$ cm/sec^2; reference altitude, $z_o = 21.3$ km
6. Baroswitch calibration: ascent 36.5 mm Hg; descent 45.0 mm Hg.
7. Baroswitch altitude: ascent 20.8 km; descent 19.5 km
8. Switching time: ascent (t_1) 2113:28.9 UT; descent (t_2) 2119:59.8 UT
9. Time of flight (first approximation): $(t_2-t_1) = 390.9$ sec
10. Velocity at reference altitude:

    $g'(t_2-t_1)/2 = 467.5 \times 10^{-5} \times 390.9 = 1.83$ km/sec
11. Time correction: ascent $0.5/1.83 = 0.3$ sec (add);

    descent $1.8/1.83 = 1.0$ sec (subtract)
12. Switching times (corrected): ascent (t_3) 2113:29.2 UT;

    descent (t_4) 2119:58.8 UT
13. Time of flight (corrected): $(t_4-t_3) = 389.6$ sec
14. Apogee altitude: $z' = z_o + \frac{g'}{2}\left[\frac{t_4-t_3}{2}\right]^2 = 21.3 + 1.169\ 10^{-3}\ (389.6)^2 = 198.8$ km
15. Apogee time: $t' = (t_3 + t_4)/2 - 0.5$ sec = 2116:43.5 UT

is used to compute the vertical component of velocity at the reference level, as shown in line 10. The corrections to be applied to the observed switching times to bring them to the reference altitude are obtained by dividing the height error by the vertical velocity. The values given in line 11 are to be added to and subtracted from the times observed on ascent and descent respectively, giving the corrected switching times, line 12. The corrected time of flight is the difference between these two times (t_4-t_3), line 13. Apogee altitude is immediately obtained, line 14, assuming the effective value of g' determined previously. Apogee time, line 15, is determined as being 0.5 sec earlier than the mid-point of the time of flight. Comparison of altitudes and times obtained from the baroswitch with those obtained by radar skin-track, in earlier flights, indicates that the probable error in altitude is $\pm$ 0.5 km and in time is $\pm$ 0.5 sec.

Knowing the apogee altitude z' and time t' the trajectory (altitude z versus time t) is easily computed using the formula

$$z = z' - \frac{g'}{2}(t-t')^2.$$

The calculation is convenient for a desk computer. The first six lines of the tabulation for the trajectory of Nike-Apache 14.92 are shown in Table B-2.The trajectory is then plotted and a smooth curve drawn through the points. It is found that the ten-second interval of the computation is sufficient.

TABLE B-2

COMPUTATION OF TRAJECTORY

Rocket: Nike-Apache 14.92

Constants used: $\frac{g'}{2} = 4.675\ 10^{-3} \text{km/sec}^2$;

$z' = 198.8$ km;

$t' = 2116{:}43.5$ UT

t	$\lvert t-t' \rvert$	$\lvert t-t' \rvert^2$	$\frac{g'}{2}\lvert t-t' \rvert^2$	z
UT	sec	sec^2	km	km
2113:30	193.5	$3.744\ 10^4$	175.0	23.8
40	183.5	3.367	157.4	41.4
50	173.5	3.010	140.7	58.1
2114:00	163.5	2.673	125.0	73.8
10	153.5	2.356	110.1	88.7
20	143.5	2.059	96.3	102.5
etc.	etc.	etc.	etc.	etc.